Discover Applied Sciences

Research

Evaluation of the strength performance and microstructural properties of different based metakaolin blended cements containing greenly synthesized nanosilica

Akeem Ayinde Raheem[1] · Rasheed Abdulwahab[2,3] · Bolanle Deborah Ikotun[2] · Ezekiel Adeyemi Adetoro[4]

Received: 20 November 2023 / Accepted: 15 April 2024
Published online: 01 May 2024
© The Author(s) 2024 OPEN

Abstract
The drive towards improving the properties of cement composite thus making it eco-friendly, sustainable, and durable, has been the focus of the construction industry. Kaolin is one of the pozzolans that have been investigated in recent times, but its reactivity is influenced by its source. In addition, the problem of homogenous mixing onsite and early strength development of pozzolana blended cement are evident. This research focused on the strength and microstructural properties of factory-produced metakaolin blended cement incorporated with green nanosilica. Kaolin samples were obtained from three locations and calcinated at 700 ℃ for 1 h. Metakaolin was interground with 10% Portland Limestone Cement (PLC) clinker at the factory. Binder-sand ratio (1:3) with a water-binder ratio of 0.5 was adopted for batching the mortar. Nanosilica was added to the mortar at: 1, 2, 3, 4, and 5%, respectively. Prisms of 40 × 40 × 160 mm were cast and cured for 3, 7, 14, 28, 56, 90, 180, 270, and 365 days, respectively. The flexural and compressive strengths of prisms including the water absorption of cubes were evaluated. 10% MK addition enhanced the mechanical properties of the mortar with MK C having the highest enhancement. Incorporation of 1% nanosilica enhanced strengths at early and later ages, as well as refinement in the pores of the mortar with increasing nanosilica.

Article Highlights

- Intergrinding metakaolin with Portland Limestone clinker at the factory to produce metakaolin blended cement.
- Sourcing of Kaolin from three different locations as against previous work.
- The nanosilica used was synthesized using extracts of cola pod *nitida*.

Keywords Blended cement · Metakaolin · Nanosilica · Compressive strength · Flexural strength · Water absorption · Microstructure

✉ Rasheed Abdulwahab, abdulwahab.rasheed@kwasu.edu.ng; abdulr@unisa.ac.za | [1]Department of Civil Engineering, Ladoke Akintola University of Technology, Ogbomoso, Nigeria. [2]Department of Civil & Environmental Engineering and Building Science, University of South Africa, Johannesburg 1710, South Africa. [3]Department of Civil Engineering, Kwara State University, Malete, Nigeria. [4]Department of Civil Engineering, Olabisi Onabanjo University, Ago-Iwoye, Nigeria.

1 Introduction

The behaviour of mortar and concrete composites depends on the characteristics of the binding material as it plays a significant role in making the constituents to form a compact whole [1]. The production of the conventional binder (Portland Limestone Cement) is energy intensive and associated with the release of carbon dioxide into the atmosphere, which in turn has tendency of deleting the ozone layer. Thus, resulting into warming of the globe [2]. There is a need to explore the application of some materials with a tendency to exhibit supplementary cementitious properties that are friendly to the ecosystem through a reduction in the emission of carbon dioxide and other related greenhouse gases with corresponding reduction in cost of production of composites [1, 3]. These materials could be agricultural residues, industrial by-products or naturally occurring. Amongst are fly ash, rice husk ash, guinea corn ash, wood ash, neem seed ash, bone ash, silica fume, activated alum sludge, and metakaolin (MK). The addition of these Supplementary Cementitious Materials (SCMs) to PLC could be by intergrinding or onsite mixing to produce blended cements. Numerous works have been done on the use of industrial wastes and agricultural residues. It is very pertinent to focus on the applications of naturally occurring clay as a partial replacement of cement in the production of concrete composites. Metakaolin (MK) being a new category of SCM, has the advantages of improving the properties of concrete composite, and solving environmental issues on the premise of reducing the emission of carbon dioxide [4, 5].

MK is alumino silicate in nature, which is being produced as a result of the thermal transformation of kaolin clay between 700 and 850 °C. The calcination parameters (temperature and time) have significant effects on the pozzolanicity of the MK. A temperature of 700 °C and a duration of 1 h have been recommended to produce MK with a good reactivity tendency [4, 6–8]. Also, the source or location where the kaolin is obtained has an influence on the chemical compositions as well as the structural arrangements of its constituting minerals. Furthermore, this determines the characteristics or reactivity of the kaolin [9]. MK has been found to possess unique properties as compared to other pozzolans because it involves the dehydroxylation of naturally occurring kaolin clay as well as having the following attributes: enhancement in the hydration reaction of cement, dilution effects, improvement in workability, and enhancement in an early strength development of mortar or concrete [10–12].

Nanomaterials are materials having a particle size in nanometres. These materials have been reported to enhance the physicomechanical properties of cement composites at elevated temperatures [3]. The fine nature and their sizes on the nanoscale enhance the properties of mortar and concrete when incorporated into the matrix. This is being initiated during the hydration of the cement [13, 14]. The addition of nanosilica (NS) to mortar and concrete has been reported to improve the properties of the composites both in fresh and hardened states [13, 15, 16].

Numerous studies have been carried out on the application of MK as SCM in concrete industries. Abdelmelek [17] worked on flexural strength of silica fume, fly ash, and MK on hardened cement paste at elevated temperatures. It was observed that there was enhancement in the strength of MK based cement paste at elevated temperature. However, the blending of conventional cement and MK was onsite and not at the factory, kaolin clay was not sourced from different locations and no incorporation of nanosilica into the cement paste. Shafiq [18] conducted research on the effect of the addition of MK containing NS on the strength and durability performance of the concrete. The combination of 10% MK and 1% NS improved the mechanical properties and durability of the concrete. However, the influence of the source of kaolin was not considered, the blending of the MK and PLC was not factory-based, and the green method of synthesizing the nanosilica was not adopted. The work of Pratyush [19] focused on the evaluation of the strength, durability, as well as microstructural properties of MK blended cement infused with nanosilica. At 28 days of curing, the combination of 10% MK and 1% nanosilica gave the maximum compressive strength. However, the influence of the source of kaolin was not considered, the method of synthesis of the nanosilica was chemical-based and not a green method, the blending of the MK and cement was not factory- based, flexural strength and water absorption were not evaluated. Sani [20] worked on the effect of the addition of MK on the hydration properties of blended cement mortar. It was concluded that a 0.5 water-binder ratio gave better consistency of the composite. However, the MK was sourced from a location, and the blending of MK and cement was not factory- based. Water absorption, flexural, and compressive strengths of the composite were not considered. This research focused on a factory blending approach of PLC clinker with calcined kaolin obtained for three different locations towards obtaining an eco-friendly, homogenous, and sustainable binder. The objective was to investigate the mechanical properties and water absorption of metakaolin blended cement mortar containing nanosilica.

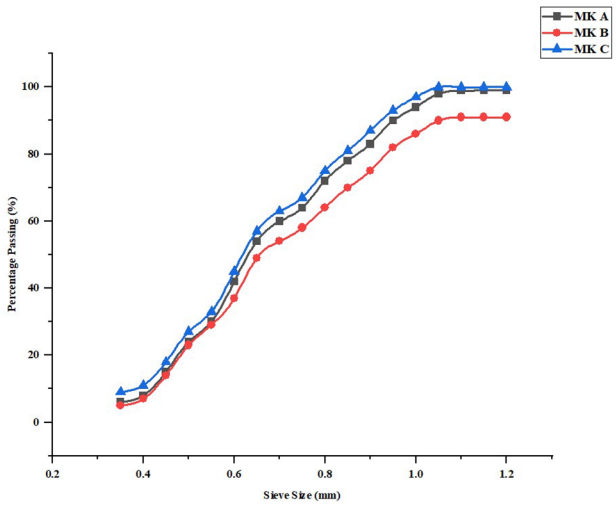

Fig. 1 Particle size distribution of metakaolin samples

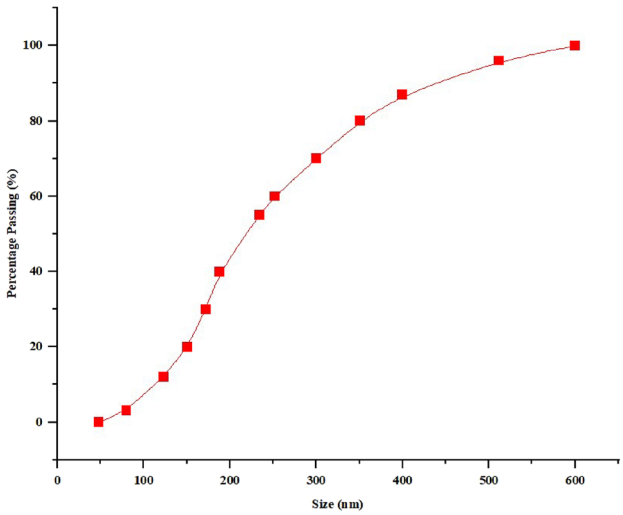

Fig. 2 Particle size distribution of nanosilica

2 Materials and methods

2.1 Materials sourcing

Kaolin clay was sourced from three (3) senatorial districts; Ijero-Ekiti on coordinates (5.056°E and 7.829°N), Ikere-Ekiti having coordinates (5.2445°E and 7.4997°N) and Isan-Ekiti on geographical coordinates (5.325°E and 7.946°N) in Ekiti State. These are represented as samples A, B, and C, respectively. PLC clinker and gypsum were obtained from Lafarge, Sagamu, Ogun State. The sand used in the production of mortar was CEN STANDARD SAND (CEN-NORMSAND, DIN EN 196-1) obtained at Lafarge, Sagamu, Ogun State, Nigeria. Cola pods were obtained from a vendor in Ogbomoso, Oyo State and the silica gotten from the Nano Biotechnology Research Laboratory, Ladoke Akintola University of Technology, Ogbomoso, Nigeria.

2.2 Methodology

The kaolin clay was transformed to MK through the process of calcination at 700 ˚C for a duration of 1 h using a muffle furnace at Department of Mechanical Engineering Workshop, Kwara State Polytechnic, Ilorin, Nigeria. Particle size distribution of the metakaolin and synthesized nanosilica were evaluated, see Figs. 1 and 2. The oxides composition

Table 1 Chemical composition of metakaolin and nanosilica. *Source*: Raheem et al. [4]

Chemical compounds	Percentage composition (%)			
	Metakaolin A (Ijero)	Metakaolin B (Ikere)	Metakaolin C (Isan)	Synthesized nanosilica
SiO_2	65.10	59.90	66.40	74.60
Al_2O_3	21.43	24.54	20.01	–
Fe_2O_3	0.18	0.59	1.01	3.60
CaO	0.00	0.066	0.090	0.01
MgO	0.00	0.00	0.00	0.70
SO_3	1.15	1.44	1.30	20.0
Na_2O	8.00	0.00	0.021	0.02
K_2O	0.00	0.00	0.33	0.15
Loss on Ignition	2.00	12.74	11.02	–
Σ (SiO_2, Al_2O_3, Fe_2O_3)	86.71	85.03	87.42	

of the MK and nanosilica as shown in Table 1 were determined using (Skyray EDX3600B X- Ray Fluorescence spectrometer, 2012). PLC clinker was interground with MK using a proportioning ratio of 90% PLC to 10% MK as shown in Table 2. The blending focused on 10% MK because it had been reported in the work of other researchers to give satisfactory performance in terms of enhancement in strengths [18, 19]. The blended cement was produced by intergrinding these two proportions thoroughly for a duration of 55 min using a mini milling machine housed at Lafarge, Sagamu Plant, Ogun State, Nigeria.

The nanosilica was synthesized by reacting a clear extract of cola pod nitida which acts as the stabilizing and capping agent with a solution of silica dioxide for a duration of 1 h at a temperature of 60 °C. This approach was adopted as performed elsewhere [21]. Thereafter, the Ultraviolet Visible (UV–VIS) spectrometry of the cola pod extract and nanosilica was investigated to determine the absorption of the particles. Also, an energy dispersive X- ray (EDX) of the nanosilica was performed to enable the determination of the elemental composition of the synthesized nanosilica. Sand-binder ratio 1:3 with water-binder ratio 0.5 was adopted in accordance with the work of other researchers elsewhere [22–25]. Also, these were adopted to produce MK blended cement mortar with nanosilica at levels of 1, 2 3, 4 and 5% by weight of the binder. Cement mortar was cast in prism size of 40 × 40 × 160 mm, cast in triplicates, and cured in water for 3, 7, 14, 28, 56, 90, 180, 270, and 365 days, respectively. The flexural strength was conducted on the prism with the application of load at the third point on the prism until failure occurred as shown in Fig. 3a. Thereafter, compressive strength was performed on the half of the prism obtained after flexural strength test as presented in Fig. 3b. The flexural and compressive strengths were performed using Toni Technik compressive and flexural strength model: 1544 in accordance with BS EN 196 [26]. Using Design Expert Software version 13, an analysis of their data was conducted to determine the relationship between flexural and compressive strength.

3 Results and discussion

3.1 UV–VIS spectroscopy of cola pod extract and nanosilica

The UV–VIS spectra for cola pod nitida extract and synthesized nanosilica are presented in Figs. 4 and 5, respectively. The peak absorption of 1.124 Abs for the extract occurred at a wavelength of 298 nm and that of the nanosilica with absorbance of 2.292 occurred at a wavelength of 236 nm. The value for the wavelength as obtained in the

Table 2 Mix proportion for each sample in terms of weight of components for charging ball mill

MIX ID	Metakaolin		OPC- Clinker		Gypsum	
	Percentage (%)	Weight (g)	Percentage (%)	Weight (g)	Percentage (%)	Weight (g)
M_0	0.00	–	95.00	3800	5.00	200
M_{10}	10.00	400	85.00	3400	5.00	200

Total weight of charge per batch was 4000 g

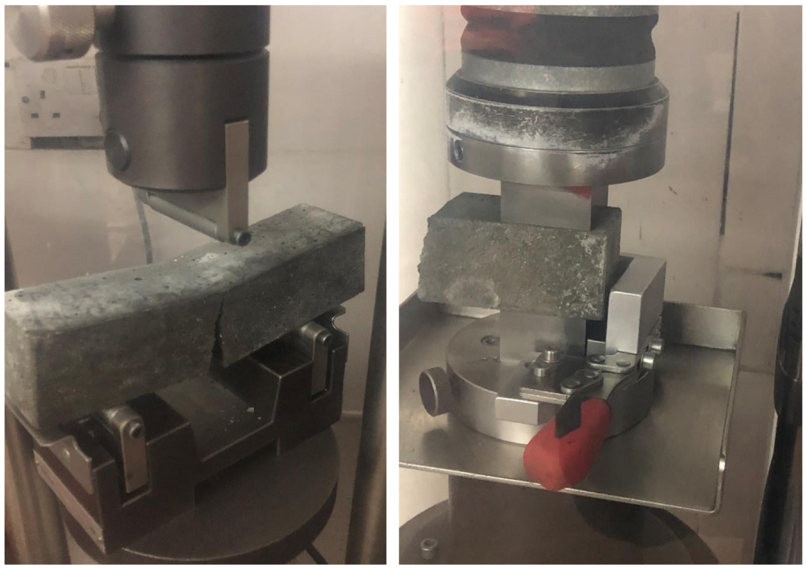

(a): Failed prism under flexural load (b): Halved prism under compressive load

Fig. 3 Prism subjected to flexural and compressive load

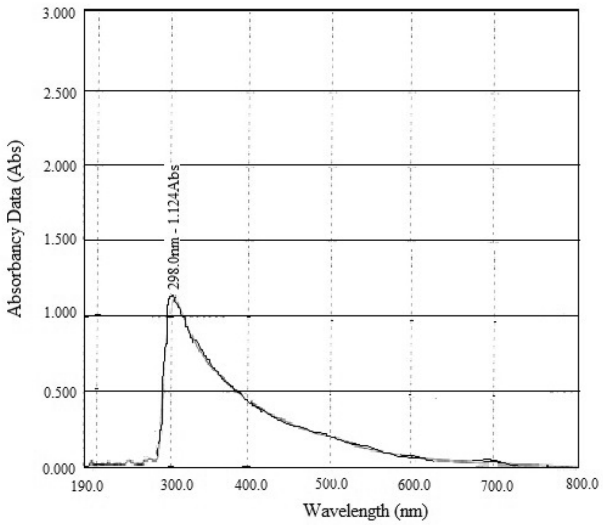

Fig. 4 UV–Vis spectroscopy of cola pod extract

case of the extract could be attributed to the double bond system contained in the cola pod extract as reported by Bisiriyu [27]. However, the wavelength of 236 nm for synthesized nanosilica was in close agreement with the value of 235 nm where a sol–gel method of synthesizing nanosilica was adopted [28] and greater than 200, 204 and 228.3 nm as reported by Al-Abboodi [29], Engku [30], Qasim [31], respectively.

3.2 EDX of nanosilica

The elemental composition of the synthesized nanosilica is presented as shown in Fig. 6. The spectrum revealed silicon as the dominating element amongst others with a relative abundance of 65.2%. The value was found to be greater than 61. 28% as obtained in the work of Behnia [32] where nanosilica was synthesized using sulphuric acid and ethanol in combination with a surfactant calcined at halved temperature of 1000 °C.

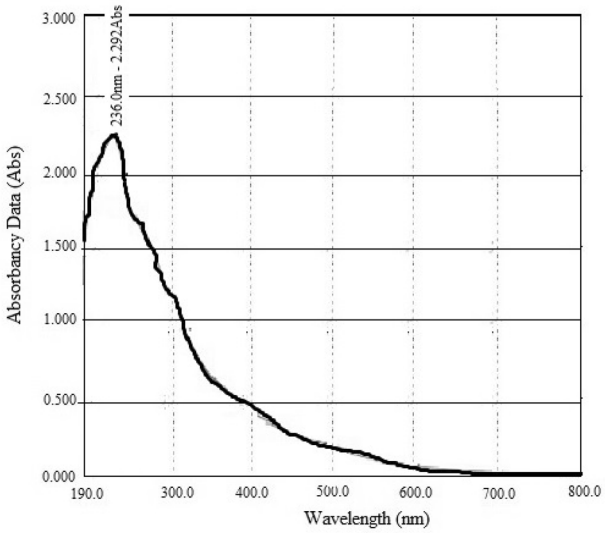

Fig. 5 UV–Vis Spectroscopy of synthesized nanosilica

3.3 Flexural strength of metakaolin blended cement mortar containing nanosilica

Flexural strength for PLC and MK blended cement mortar sourced from different locations infused with nanosilica is presented in Figs. 7, 8, 9. These figures show that flexural strength of 10% MK blended cement surpassed that of the PLC at early and later ages. This agrees with the work of Regina [33], Menshaz [34]. The addition of nanosilica to the blended cement mortar up to a level of 1% was observed enhance the flexural strength at both early and later curing ages. This agrees as reported in other research, where 1% nanosilica addition to cement mortar and concrete gave maximum flexural strength [18, 19, 35, 36]. The flexural strength was observed to reduce as the percentage of nanosilica increased from 2 to 5%. The reduction in strength may be due to the formation of excessive nucleation sites outweighing the atoms reacting together. In addition, the problem of adequate dispersion of the nanosilica could lead its agglomeration [37, 38]. Figure 9 shows the flexural strength of MK blended cement obtained from sample C, which surpassed that of Figs. 6 and 7 (representatives of samples A and B, respectively). This is an indication that the source of kaolin clay had an influence on the bending strength of MK blended cement mortar.

3.4 Compressive strength of metakaolin blended cement mortar containing nanosilica

Figures 10, 11, 12 show the compressive strength of PLC, MK blended cement with and without nanosilica for samples A, B and C, respectively. These Figures revealed the compressive strength for PLC at the end of 365 days to be 65. 75 N/mm^2. MK blended cement mortar at same curing ages ranged 67.98–70.13 N/mm^2. The result showed enhancement in compressive strength of MK blended cement mortar as compared to that of PLC. This agrees with the findings of Menshaz [34], Alonge [39], Naresh [40]. The incorporation of nanosilica to MK blended cement mortar was observed to initially increase the compressive strength and decreased with subsequent addition of nanosilica; 1% nanosilica given the maximum compressive strength. This is as reported elsewhere [18, 19, 35, 36]. The compressive strength was observed to decrease as the percentage of nanosilica was increased from 2 to 5%. The reduction may be because of excessive nucleation site formation and problem of dispersion of more content of nanosilica [37, 38]. The trend of result as obtained in this work is in contrary to the findings of Ltifi [41] where the influence of nanosilica was examined on the behaviour of PLC mortar. It was observed that the compressive strength increased as the percentage of nanosilica was increased between 3 and 10%. This may be because the binder used was PLC alone and not pozzolana blended cement. Figures 10, 11, 12 revealed the compressive strengths of MK blended cement mortar obtained from different locations with addition of nanosilica. Figure 12 showed strength of sample C which surpassed Figs. 10 and 11, samples A and B, respectively. This is an indication of influence of location of MK on the strength of the blended cement mortar.

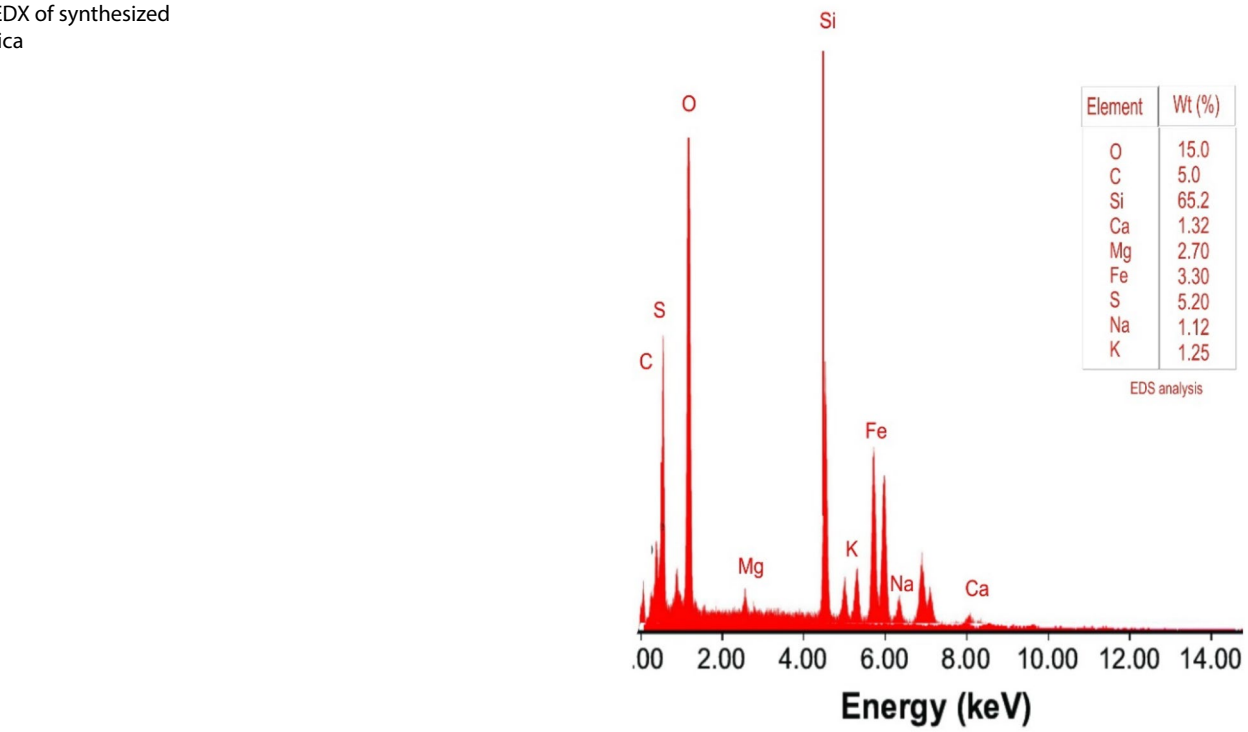

Fig. 6 EDX of synthesized nanosilica

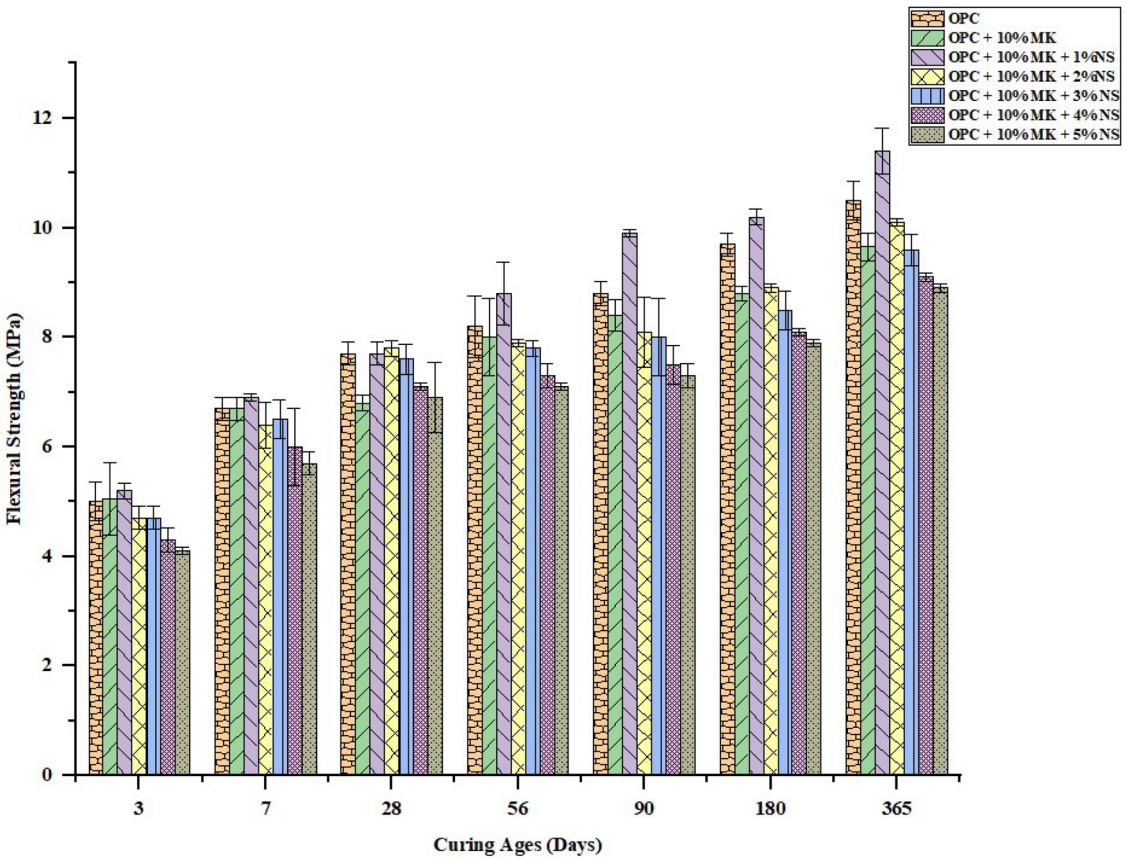

Fig. 7 Flexural strength of sample A blended cement incorporated with nanosilica

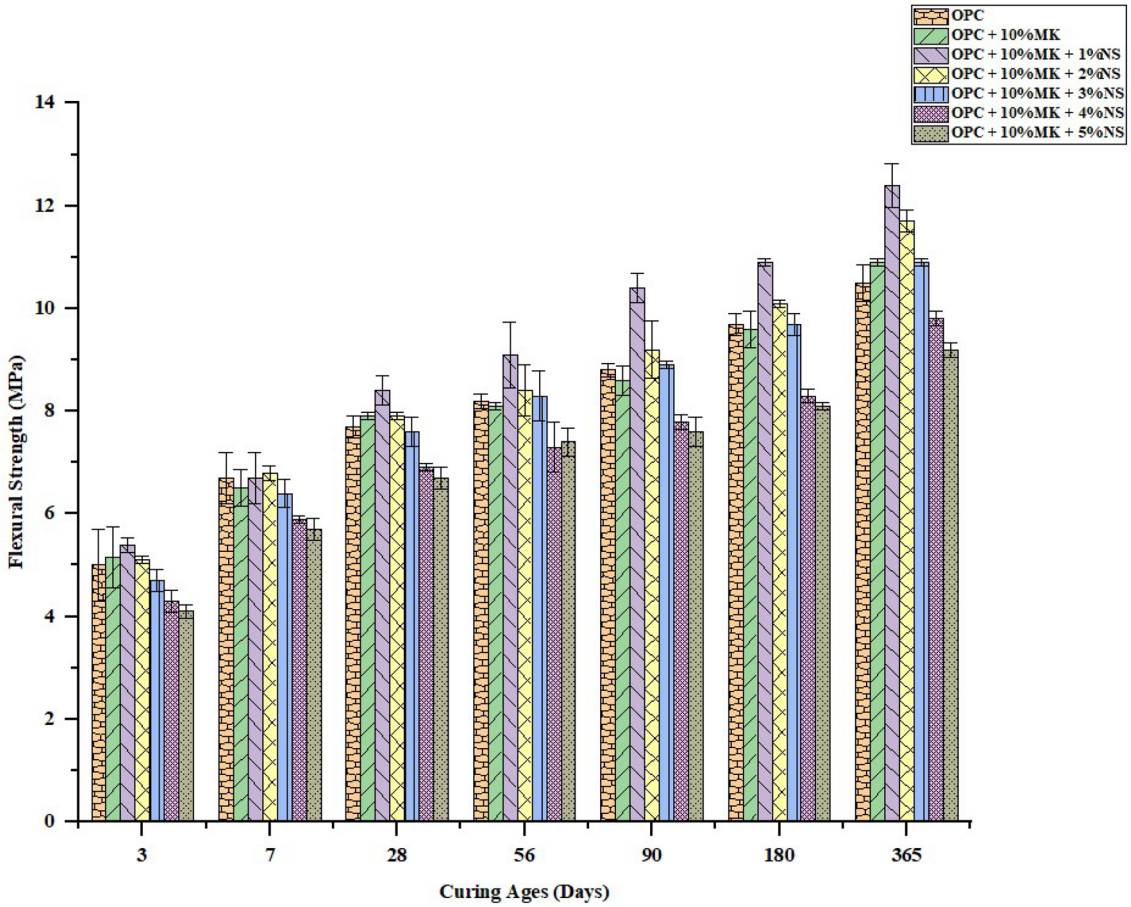

Fig. 8 Flexural strength of sample B blended cement incorporated with nanosilica

3.5 Relationship between flexural and compressive strength of metakaolin blended cement mortar with nanosilica

The flexural and compressive strengths are parameters that determine the viability and behavioural pattern of a material under loading or while in use. The need to establish the relationship between the two dependent variables is important as it enhances the prediction or determination of one unknown parameter if the other is evaluated or determined.

3.5.1 Overview of the experimental setup

Using the response surface methodology of central composite design on Design expert software version 13 (DOEv13) [42], the experimental design was completed. Two selected parameters were added to the CCD's empirical domain in order to generate experimental sets. With no blocks and responses in the form of flexural and compressive strength, the polynomial (fifth) design model was used. The two parameters that were chosen considering their levels' ranges, the design generated fifty-seven (57) runs; the findings showed that no performance changes were applied to the responses as presented in Table 3.

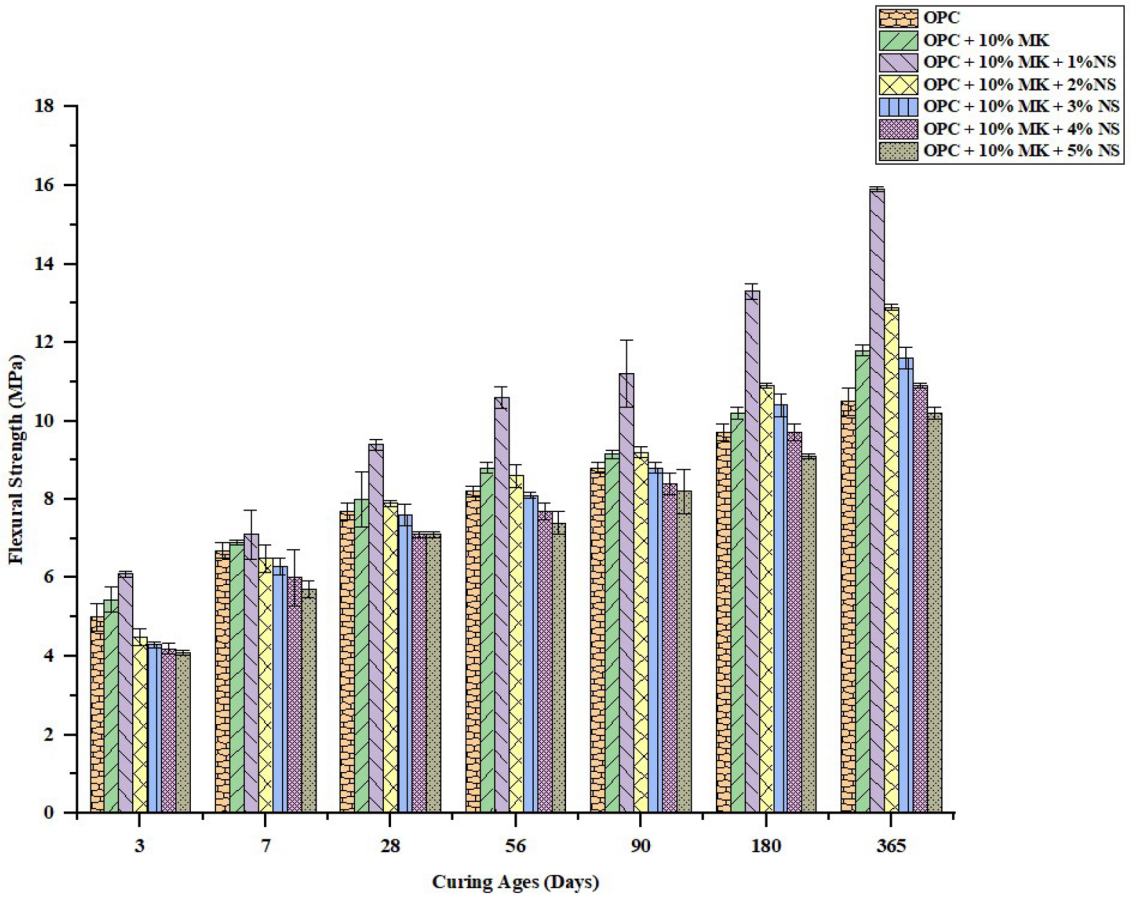

Fig. 9 Flexural strength of sample C blended cement incorporated with nanosilica

3.5.2 Responses to experimental details

The responses' extreme and minimal frequencies, along with the corresponding runs for each factor, are summarized in Table 4. It was found that the anticipated ranges for compressive and flexural strength were 23.812 to 76.731 N/mm^2 and 6.624 to 15.939 N/mm^2, respectively.

3.5.3 Overview and modification parameters for the model

Table 5 shows the model overview and modification parameters for the responses of compressive and flexural strength. The standard deviation displays the error, or degree of variation, between the experimental and true values. They were in the range of 0.297 and 0.432 for both responses. They had expected (r^2) values ranging from 0.933 to 0.952, whereas their fitted (R^2) values were between 0.9575 and 0.9744. According to [42, 43], all expected (r^2) values agreed with the fitted (R^2) values for both responses because their differences were less than 0.2.

The range of values for the signal-to-noise ratio measured with tolerable accuracy is 28.758–42.828. These showed that both models had sufficient signals to explore the design space, as evidenced by their appropriate precision ratings exceeding 4.0. Additionally, all of the models' p values were less than 0.05 ($p < 0.05$), and their F values (i.e. $p < 0.0001$), demonstrating their importance with no complacency [42, 43].

3.5.4 ANOVA (variance's analysis)

The summary of surface polynomial (fifth) response models' Analysis of Variance (ANOVA) results of flexural and compressive strengths is displayed in Table 6. The model was significant, as indicated by its F-value of 107.47. There is likelihood of noise producing high Model F at about 0.01%. If the value of *P* (i.e., 95% confidence interval) was less than 0.05, model

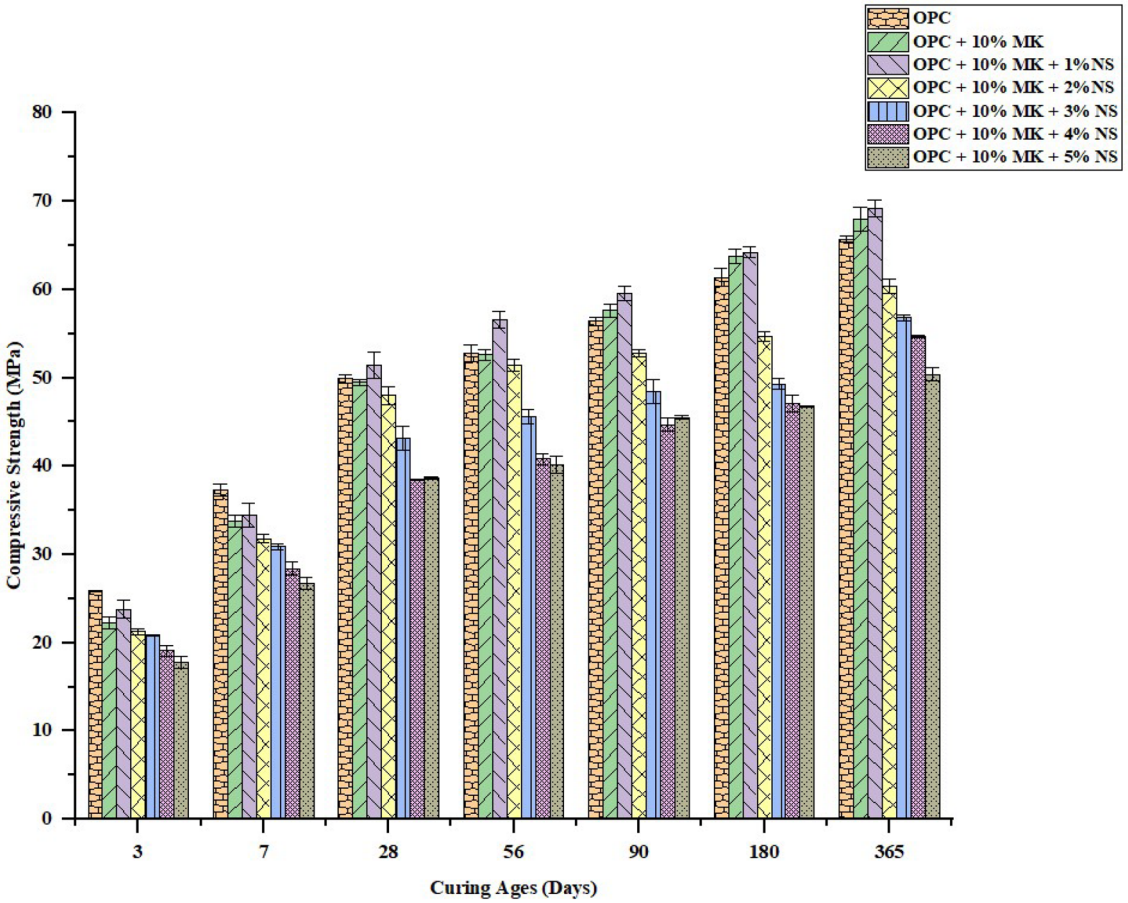

Fig. 10 Compressive strength of sample A blended cement incorporated with nanosilica

parameters were considered highly meaningful; if the value was more than 0.10, the parameters were not meaningful. The model terms become more important when the absolute F-value increases and the P-value decreases. In this instance, major important model parameters were A, B, A^2, B^2, A^2B, A^3, B^3, A^3B, A^4, A^4B, A^5, and B^5. Other model parameters needed to preserve the hierarchy [42, 43].

3.5.5 Equations of the model

Equations (1) and (2) are the equations for regression that were used to forecast the responses i.e. the flexural and compressive strength (ultimate experimental models in the form of coded components). A negative sign before the words denotes an opposing impact, whereas a plus sign denotes a cooperative impact on the observed response. B is the curing age (days), and A is the MK C.

$$\begin{aligned}\text{Response (Flexural Strength)} = {} & 10.62 - 1.79A + 5.33B - 1.61AB + 4.36A^2 - 3.77B^2 + 2.49A^2B - 0.47AB^2 \\ & - 5.02A^3 - 17.01B^3 + 0.3284A^2B^2 + 1.81A^3B - 0.33AB^3 - 5.01A^4 + 1.59B^4 \\ & - 0.54A^3B^2 - 0.15A^2B^3 - 2.94A^4B + 0.74AB^4 + 6.35A^5 + 15.18B^5\end{aligned} \quad (1)$$

$$\begin{aligned}\text{Response (Compressive Strength)} = {} & 62.55 - 21.42A + 29.57B - 2.82AB + 3.24A^2 - 17.72B^2 + 7.67A^2B + 3.00AB^2 \\ & + 19.44A^3 - 125.93B^3 + 0.06A^2B^2 + 2.92A^3B - 1.85AB^3 - 1.85AB^3 - 6.23A^4 \\ & + 3.28B^4 - 6.14A^3B^2 - 4.45A^2B^3 - 3.44A^4B + 4.92AB^4 - 4.39A^5 + 115.13B^5\end{aligned} \quad (2)$$

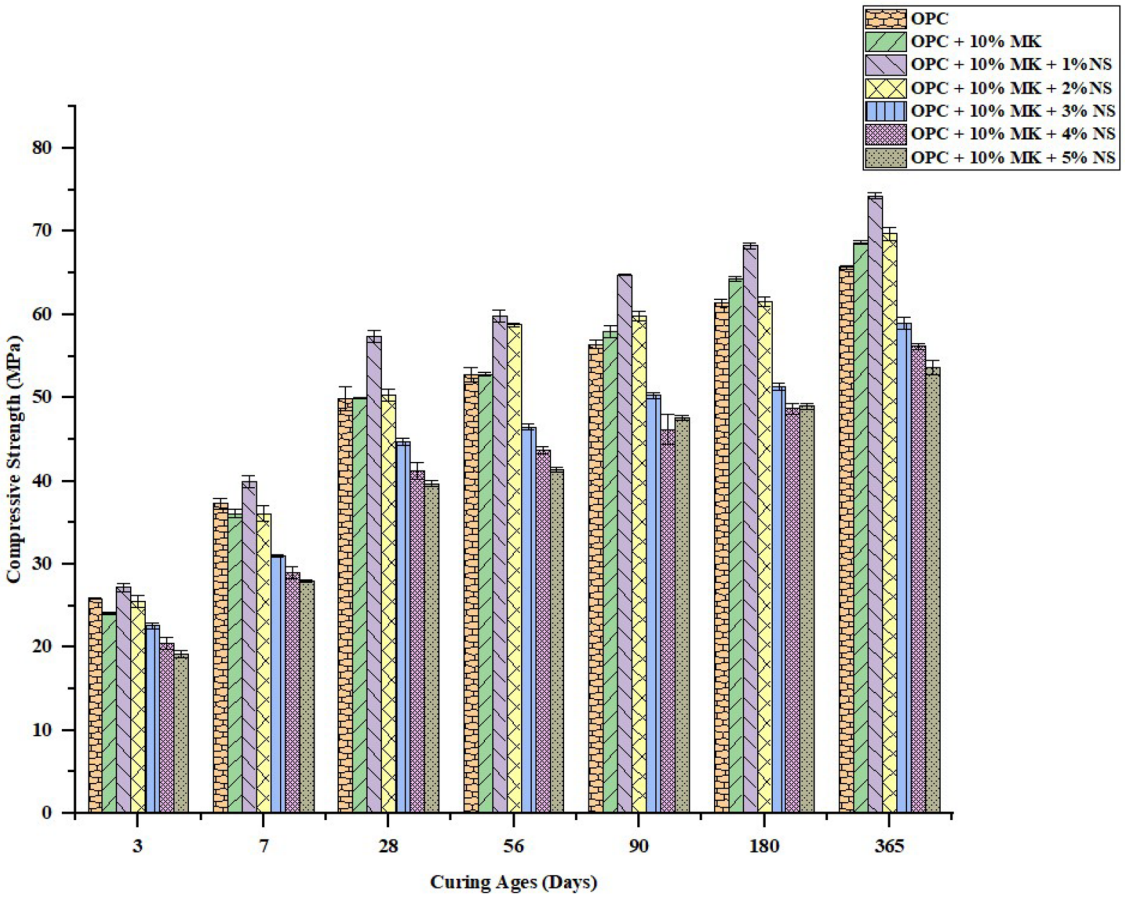

Fig. 11 Compressive strength of sample B blended cement incorporated with nanosilica

3.5.6 Model charts

Figure 13 shows the relationship between the flexural and compressive strength of MK blended cement mortar infused with nanosilica at a level of 1%. The curve gave a coefficient of determination (R^2) value of between 0.945 and 0.955 with a polynomial geometry adopted as the best curve fitting. The responses' anticipated and experimental values agreed quite well, with the greatest r^2 value being 0.952. There was no difference between the true and expected values where flexural and compressive strength values met. Nonetheless, the values were either positive (flexural > compressive strength), indicating that the true values exceeded what was expected, or negative, indicating that the true values were lower or vice versa. These charts demonstrated good residual normality. The correlation between the true and expected values of the responses was supported by the r^2 values in Table 5.

This geometry is in line with the findings of Zhang [44]. However, the value of (R^2) obtained in the work of Shodolapo [45] was found to be 0.8037 where quadratic pattern of curve was adopted. The discrepancy in value may be attributed to the quadratic pattern as against the polynomial or cubic curve fittings adopted. However, the quadratic curve showed a very good correlation between the flexural and compressive strength as the value approaches unity [46]. The value of coefficient of determination obtained in this work is close agreement with 0.989 as obtained in the work of Yusuf [47] where an appropriate relationship between flexural and compressive strength of palm kernel shell concrete was investigated. The work concluded a polynomial curve fitting to be the best relationship.

Figure 14 displays the contour and 3D response area graphs for the flexural and compressive strength responses as functions of the MK sourced at location C and Curing age. The determined response surface forecasts were used to verify the models. The hot (main) reaction zone made by the graphs encompassed all the forecasts. The figure's

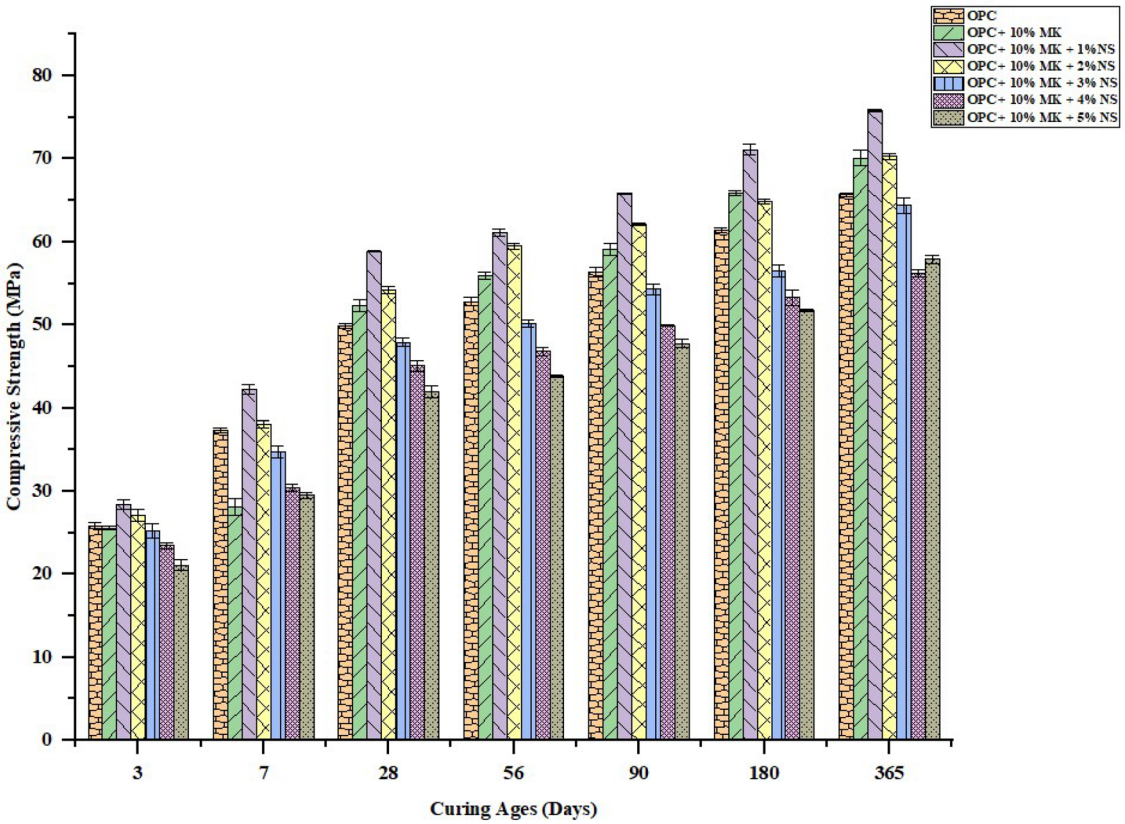

Fig. 12 Compressive strength of sample C blended cement incorporated with nanosilica

red colour denotes the primary reaction zone, green denotes a potential reaction zone (meaning that reaction can occur there even in the presence of impurities), and blue denotes a cold reaction zone (meaning that though there may be a reaction in this area, it is not very likely). The models' four edges natures show the important role of both aspects in the processes. Equations (1) and (2) show how the graph types reaffirmed the models' polynomial structure. Figures 13 and 14 showed how compressive strength increases with flexural strength and vice versa.

3.5.7 Optimization

According to Table 7, the optimal results for flexural and compressive strength was 15.939 and 76.731 N/mm^2, respectively. Maximum compressive strength and maximum flexural strength were obtained with these results. Their standard error was sufficiently small, ranging from 0.282 to 1.943%. Given that it was less than 5%, the results were good.

3.6 Water absorption of metakaolin blended cement mortar containing nanosilica

The water absorption of blended cement obtained from different kaolin locations with addition of 5% nanosilica at the end of 28 days for samples A, B, and C are 1.01, 1.20 and 1.03% respectively as presented in Fig. 15. These values were observed to be lower than 1.72, 1.65, and 1.56% MK blended cement of samples A, B, and C, respectively. Also, the water absorption for PLC at the same curing age was found to be 1.98%. The graph revealed a reduction in water absorption as the percentage of nanosilica increased. This may be attributed to the reduction in the pores of the hardened mortar which is an indication of the pore refinement tendency exhibited by nanosilica [48, 49].

Table 3 Overview of experimental setup

Parameter	Code	Unit	Level		Response	Unit	Analysis	Transform	Model
			Low (− 1)	High (+ 1)					
MK C	A	%	0	5	Flexural & Compressive strength	N/mm^2	Polynomial	None	Fifth
AGE	B	day	3	365					

Table 4 Overview of the responses' high and low values

Response	Extreme	Run	Minimal	Run
Flexural strength	15.939	53	6.624	52
Compressive strength	76.731	56	23.812	52

Table 5 Details on the model's fit and overview for compressive and flexural strength

Response	Std. Dev	Fitted R^2	Expected r^2	Tolerance Accuracy	F-value	*p*-value
Flexural Strength	0.4315	0.9744	0.9520	42.828	10.65	< 0.0001
Compressive Strength	0.297	0.9575	0.9325	28.7579	8.39	< 0.0001

Table 6 ANOVA for the compressive and flexural strength

Source	Sum of squares	Mean square	F-value	*p*-value
Model	400.1	20.01	107.47	< 0.0001*
A-MK C	1.08	1.08	5.81	0.0211*
B-AGE	7.68	7.68	41.27	< 0.0001*
AB	1.54	1.54	8.25	0.0068*
A^2	5.54	5.54	29.75	< 0.0001*
B^2	1.8	1.8	9.67	0.0036*
A^2B	0.8418	0.8418	4.52	0.0404*
AB^2	0.0213	0.0213	0.1146	0.7369
A^3	0.7928	0.7928	4.26	0.0463*
B^3	5.47	5.47	29.4	< 0.0001*
A^2B^2	0.1101	0.1101	0.5913	0.4469
A^3B	3.82	3.82	20.5	< 0.0001*
AB^3	0.0786	0.0786	0.4223	0.5199
A^4	10.03	10.03	53.91	< 0.0001*
B^4	0.428	0.428	2.3	0.1382
A^3B^2	0.0891	0.0891	0.4786	0.4935
A^2B^3	0.0063	0.0063	0.034	0.8548
A^4B	2.2	2.2	11.8	0.0015*
AB^4	0.0852	0.0852	0.4578	0.503
A^5	2.22	2.22	11.94	0.0014*
B^5	7.18	7.18	38.57	< 0.0001*

*Important

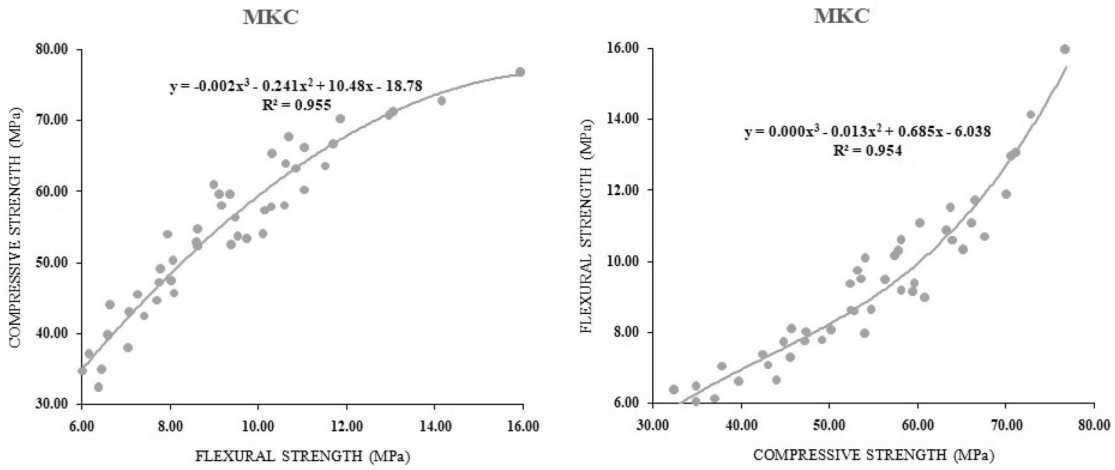

Fig. 13 Relationship between flexural and compressive strength of sample C blended cement containing nanosilica

3.7 Microstructure of OPC and metakaolin blended cement

Figure 16 shows the SEM micrograph of OPC and that of MK blended cements. The MK blended cement shows micrograph that is plate like in nature. This agrees with the findings as obtained elsewhere [50–52]. Figure 16c and d show blended cement with predominance of plate like structure. This is an indication of high amorphous tendency exhibited by the duo when compared to Fig. 16a. This may be attributed to the effect of the source of kaolin on the characteristics of the binder.

3.8 Microstructure of metakaolin blended cement mortar containing nanosilica

The pores in the MK blended cement mortar in the hardened state were observed to reduce with addition of 1% nanosilica as presented in Fig. 17. The micrographs showed denser medium with C–S–H bonding enhanced due to the incorporation of nanosilica as compared with that of MK blended cement shown in Fig. 16. The refinement exhibited is in agreement with some previous work [33, 53].

4 Conclusion

At the end of this research, the following conclusions were drawn:

- Intergrinding of 10% MK with PLC shows enhancement in flexural and compressive strengths as compared to the conventional PLC binder.
- The source of kaolin clay influenced the reactivity of MK, and consequently, the properties of MK blended cement.
- The compressive and flexural strengths of MK blended cement mortar were enhanced at a low percentage of nanosilica addition.
- The high wavelength recorded in the synthesized nanosilica could be attributed to the conjugate double bond exhibited by the cola pod extract.
- The addition of nanosilica enhanced the pore fineness of hardened metakaolin blended cement mortar.
- Addition of nanosilica reduced the water absorption of metakaolin blended cement mortar with 5% nanosilica having the least water absorption.

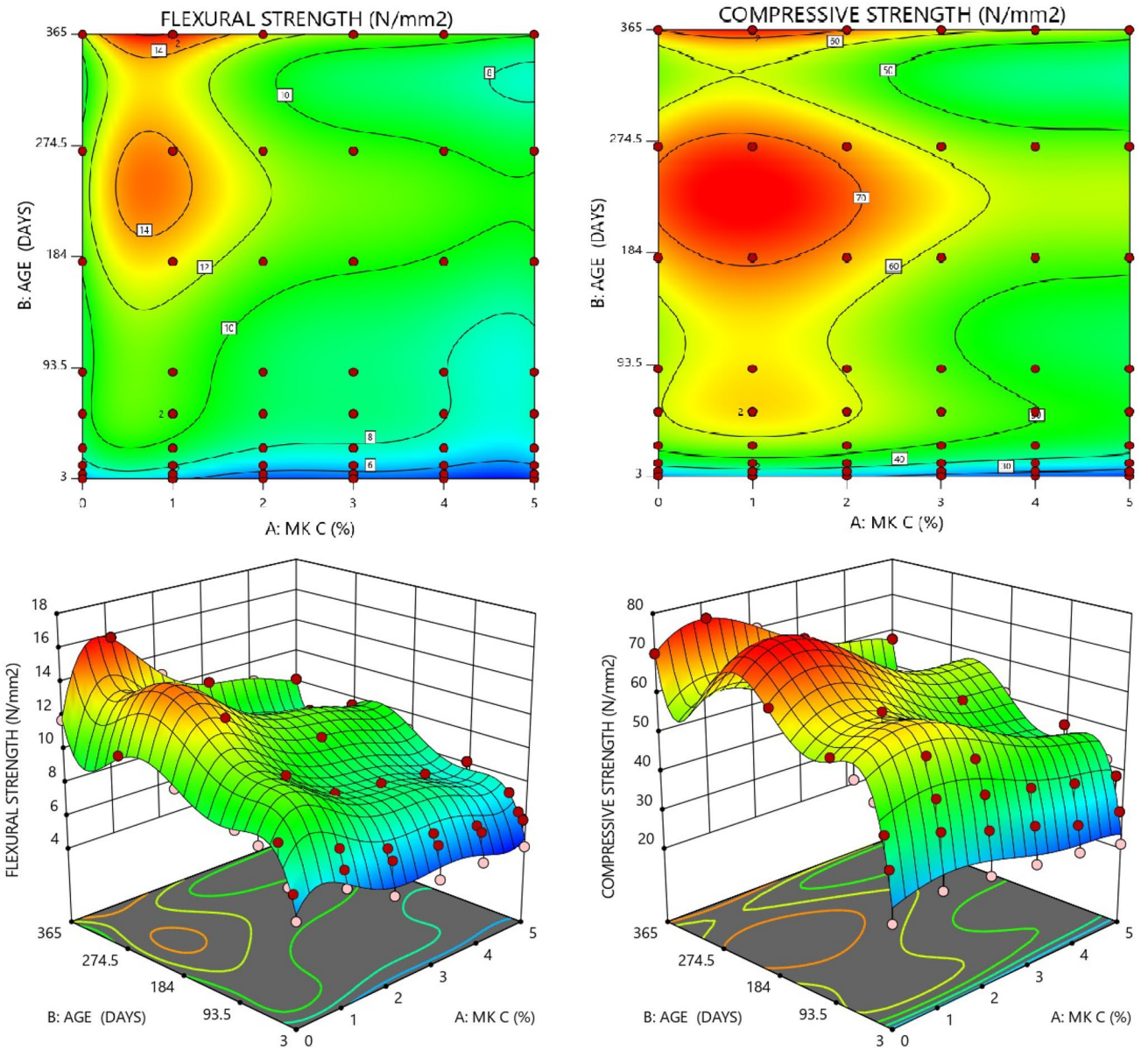

Fig. 14 3D Response Surface and Contour Graphs of flexural and compressive strength models

Table 7 Optimal result for flexural and compressive strength

MK C (%)	AGE (day)	Flexural strength (N/mm^2)	Std. error (%)	Compressive strength (N/mm^2)	Std. error (%)
1.0004	365	15.939	0.282	76.731	1.943

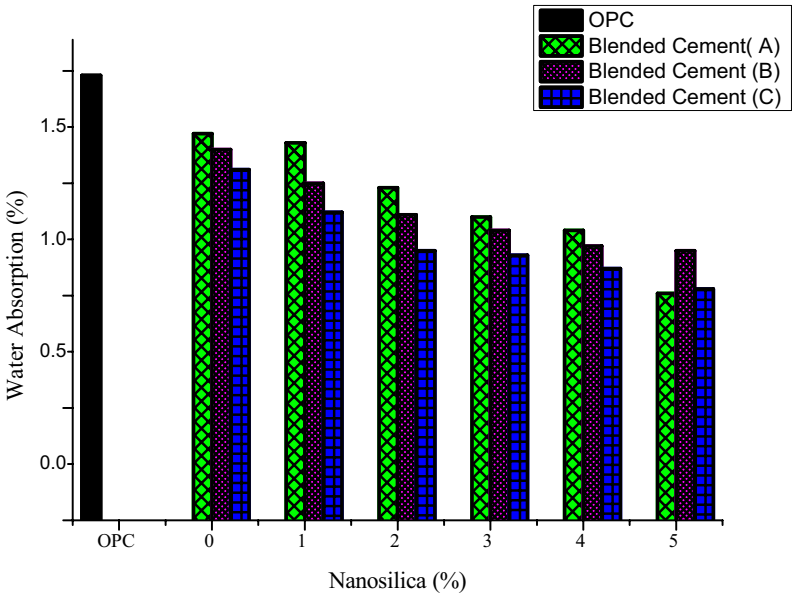

Fig. 15 Water Absorption of Blended Cement Mortar containing nanosilica at 28 days

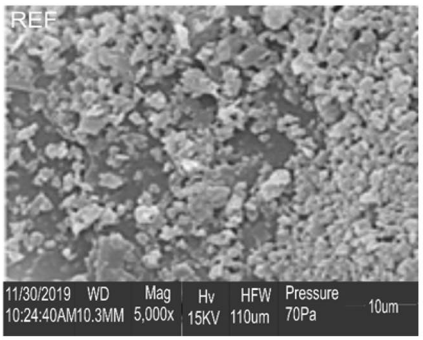

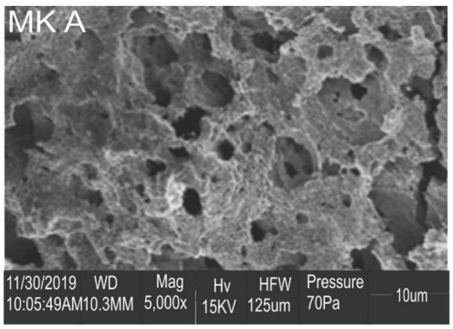

a: SEM micrograph of OPC

b: micrograph of MK A blended cement

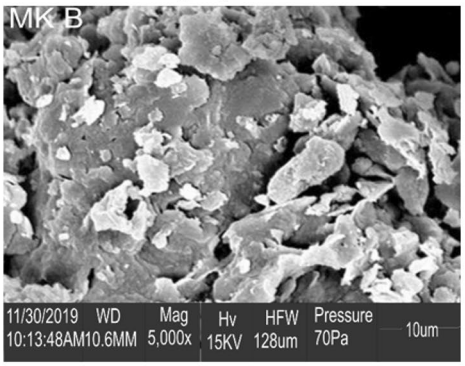

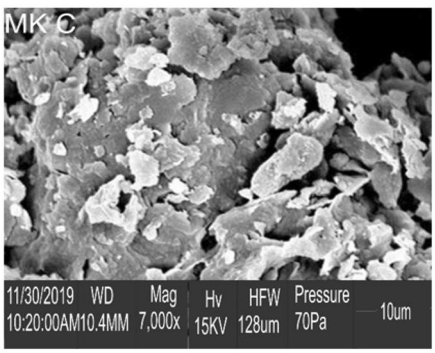

c: micrograph of MK B blended cement

d: micrograph of MK C blended cement

Fig. 16 SEM micrographs of OPC and metakaolin blended cement

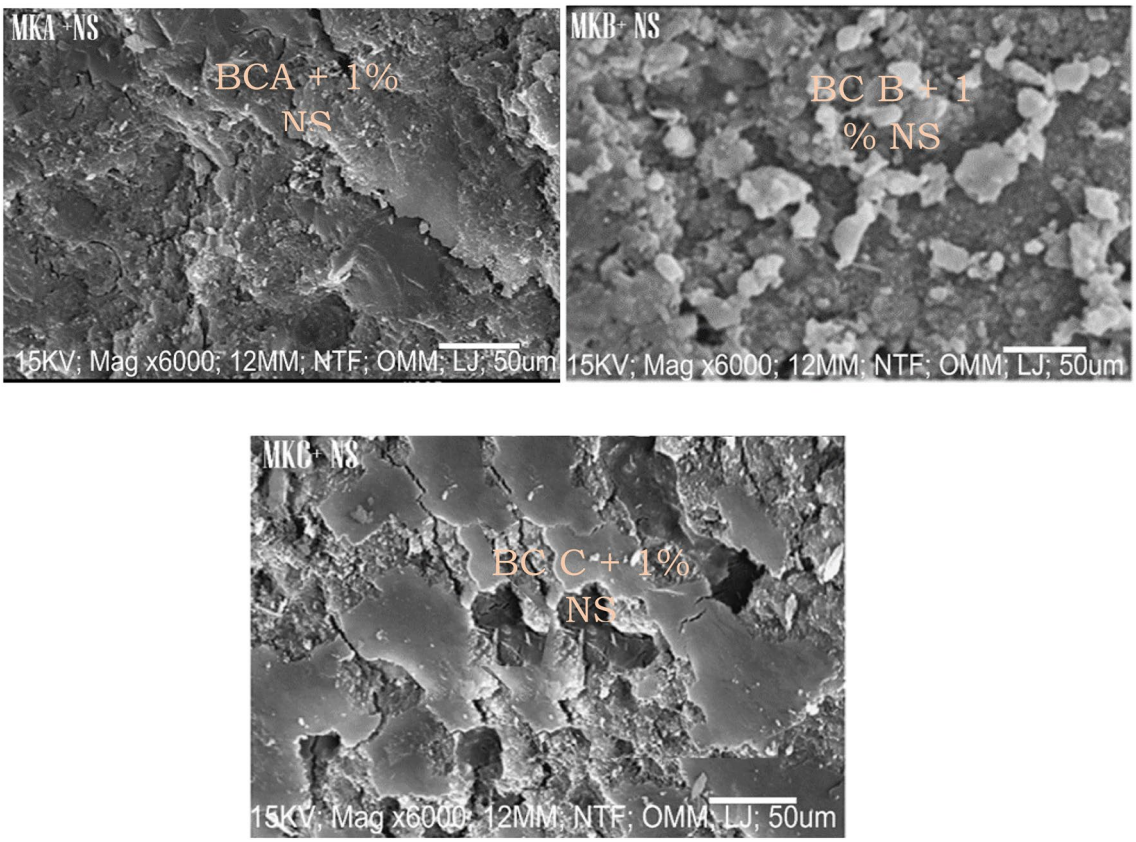

Fig. 17 SEM micrographs metakaolin blended cement mortar with 1% nanosilica

Acknowledgements The authors acknowledged the supports members of LAUTECH Nano^{+}Research group, LAUTECH, Ogbomoso, Nigeria and Technical staff in the Laboratory of the West African Portland Cement, Lafarge, Sagamu, Ogun State, Nigeria.

Author contributions AAR: Conceptualization, Supervision, Methodology, Investigation, Writing- review & editing, Validation. RA: Conceptualization, Data curation, Formal analysis, Funding acquisition, Investigation, Methodology, Resources, Visualization, Writing- original draft. BDI: Formal analysis, writing- review & editing. EAA: Formal analysis, writing- review & editing. The authors acknowledged the supports members of LAUTECH Nano^{+}Research group, LAUTECH, Ogbomoso, Nigeria and Technical staff in the Laboratory of the West African Portland Cement, Lafarge, Sagamu, Ogun State, Nigeria.

Funding Open access funding provided by University of South Africa.

Data availability All data used in this manuscript do not involve human/living organisms and were results of laboratory investigations carried out on the application of metakaolin blended cement. The procedures to achieving these results have been extensively described under the methodology. No data were sourced online or replicated from previous studies; all information is primary and, on this note, no available link to any data. In addition, appropriates references have been duly cited in the work to corroborate the findings of previous work done.

Declarations

Competing interests The authors declare no competing interests.

Open Access This article is licensed under a Creative Commons Attribution 4.0 International License, which permits use, sharing, adaptation, distribution and reproduction in any medium or format, as long as you give appropriate credit to the original author(s) and the source, provide a link to the Creative Commons licence, and indicate if changes were made. The images or other third party material in this article are included in the article's Creative Commons licence, unless indicated otherwise in a credit line to the material. If material is not included in the article's Creative Commons licence and your intended use is not permitted by statutory regulation or exceeds the permitted use, you will need to obtain permission directly from the copyright holder. To view a copy of this licence, visit http://creativecommons.org/licenses/by/4.0/.

References

1. Raheem AA, Abdulwahab R, Kareem MA. Incorporation of metakaolin and nanosilica in blended cement mortar and concrete- a review. J Clean Prod. 2021;290:1–12. https://doi.org/10.1016/j.jclepro.2021.125852.
2. Odeyemi SO, Abdulwahab R, Giwa ZT, Anifowose MA, Odeyemi OT, Ezenweani CF. Effects of combining maize straw and palm oil fuel ashes in concrete as partial cement replacement in compression. Trends Sci. 2021;18(19):1–11. https://doi.org/10.48048/tis.2021.29.
3. Mohamed OA, El-Gamal SMA, Farghali AA. Utilization of alum sludge waste for production of eco-friendly blended cement. J Mater Cycles Manag. 2022;24:949–70. https://doi.org/10.1007/s10163-022-01369-x.
4. Raheem AA, Abdulwahab R, Kareem MA. Characterization and effects of nanosilica on consistency and setting times of metakaolin blended cement mortar. Nano Plus Sci Technol Nanomat. 2021;2:66–75. https://doi.org/10.48187/stnanomat.2021.2.004.
5. Adetoro EA, Abdulwahab R, Adetoro OD, Ojoawo SO, Naik P. Treatment effect on reactivity of metakaolin Using *Azadirachta Indica* Bark activated carbon. Mater Today Proc. 2023;88:119–27. https://doi.org/10.1016/j.matpr.2023.05.620.
6. Akinyele JO, Odunfa SO, Famoye AA, Kuye SI. Structural behaviour of metakaolin infused concrete structure. Niger J Technol. 2017;36(2):331–8.
7. Ayininuola GM, Adekitan OA. Characterization of Ajebo Kaolinite Clay for production of natural pozzolan. Int J Civ Environ Struct Constr Eng. 2016;10:1212–9.
8. Amer MI, Khalid AA. Effect of temperature on the pozzolanic properties of metakaolin produced from iraqi kaolin clay. AL- Fatih J. 2008;4(32):268–85.
9. Bello AM, Ismail IM, Yalwa IR. Physicochemical evaluation of industrial potentialities of getso kaolin. ChemSearch Journal. 2017;8(2):16–21.
10. Sabir BB, Wild S, Bai J. Metakaolin and calcined clays as pozzolans for concrete: a review. Cement Concr Compos. 2001;23(6):441–54.
11. Chandak MA, Pawade PY, Influence of Metakaolin in Concrete Mixture - A Review. International Journal of Engineering Science, 37–41. (2018)
12. Moodi F, Ramezanioanpour AA, Safavizadeh AS. Evaluation of the optimal process for the thermal activation of kaolins. ScientiaIranica. 2011;18(4):906–12. https://doi.org/10.1016/j.scient.2011.07.011.
13. Sanchez F, Sobolev K. Nanotechnology in concrete- a review. Constr Build Mater. 2010;24(11):2060–71. https://doi.org/10.1016/j.conbuildmat.2010.03.014.
14. Mahender B, Ashbok B. Effects of nanosilica on the compressive strength of concrete. Int J Prof Eng Stud. 2017;3(2):222–6.
15. Jinfeng S, Zhiqiang X, Weifeng L, Xiaodong S. Effects of nanosilica on the early hydration of alite-sulphoaluminate cement. Nanomaterials. 2017;7(102):1–15.
16. Ahmed AA, Tarek ME, Nagwa IA. Thermal durability of OPC pastes admixed with nano iron oxide. Housing Build Nat Res Center J. 2015;11(2):299–305. https://doi.org/10.1016/j.hbrcj.2014.04.002.
17. Abdelmelek N, Lubloy E. Flexural strength of silica fume, fly ash and metakaolin of hardened cement paste after exposure to elevated temperatures. J Therm Anal Calorim. 2021. https://doi.org/10.1007/s10973-021-11035-3.
18. Shafiq N, Kumar R, Zahid M, Tufail RF. Effects of modified metakaolin using nanosilica on the mechanical properties and durability of concrete. Materials. 2019;12(14):1–22. https://doi.org/10.3390/ma12142291.
19. Pratyush K, Sofi A Study of Microstructural and Durability Properties of Nanosilica and Metakaolin Based Cement Mortar. In: 9th International Conference of Materials Processing and Characterization, (2018), 1–10
20. Sani ND, Mukesh K, Saxena SK, Singh NB. Hydration reaction of metakaolin blended cement in the presence of superplasticizer. Int J Curr Res. 2017;9(4):48686–90.
21. Raheem AA, Lateef A, Akinola PO, Adeniyi AA, Yusuf SO. Influence of nanosilica on workability and compressive strength of wood ash cement concrete. LAUTECH J Civ Environ Stud. 2019;2(1):22–8.
22. Hui L, Hui-gang X, Jin-ping O. A study on mechanical and pressure sensitivity properties of cement mortar with nano-phase material. Cem Concr Res. 2004;34:435–8.
23. Sani ND, Mukesh K, Saxena SK, Singh NB. Hydration reaction of metakaolin blended cement in the presence of superplasticizer. Int Curr Res. 2017;9(4):48686–90.
24. Wang X, Effects of Nanoparticles on the Properties of Cement-based Materials. PhD Thesis, Iowa State University, Ames, Iowa, (2017) 53–54
25. Mounir L, Achraf G, Pierre M, Abdelhafid K. Experimental study of the effect of addition nanosilica on the behaviour of cement mortars. Sci Direct Proc Eng. 2011;10:900–5.
26. BS EN 196-1. Methods of Testing Cement- Part 1: Determination of Strength, British Standard Institute, 389 Chiswick High Road, London, W4 4AL, (2005) 1–33
27. Bisiriyu MT, Idris S, Aliyu HG, Muhammad AB, Sokoto AM, Abdulkarim AM. Fractionation and characterization of asphaltic and resinous fraction of natural bitumen. Commun Phys Sci. 2020;5(2):61–71.
28. Al-Shaikh Hussin SH, Al-Hamdani AH, Abdalgaffar AN. Optical and morphological characteristics of silicondioxide nanoparticles by Sol-Gel method. Int J Sci Eng Res. 2016;7(8):234–7.
29. Al-Abboodi SM, Abed Al-Shaibani EJ, Alrubai EA. Preparation and characterization of nanosilica prepared by different precipitation methods. Mater Sci Eng. 2020;978:1–13. https://doi.org/10.1088/1757-899X/978/1/01231.
30. Engku Ali EA, Matori KA, Sidek E, Zahid HAMH, Alibe IM. Effect of reaction time on structural and optical properties of porous silica nanoparticles. Digest J Nanomater Biostruct. 2017;12(2):441–7.
31. Qasim M, Ananthaiah J, Dhara S, Paik P, Das D. Synthesis and characterization of ultra fine colloidal silica nanoparticles. Adv Sci Eng Med. 2014;6:965–73.
32. Behnia B, Safardoust-Hojaghan H, Amiri O, Salavati-Niasari M, Anvari AA. High performance cement mortars-based composites with nanosilica: synthesis, characterization and mechanical properties. Arab J Chem. 2021;14:1–8. https://doi.org/10.1016/j.arabjc.2021.103338.

33. Regina K, Arunas B, Rimantas L, Jurate C. Incineration residual ash-metakaolin blended cement- effect on cement hydration and properties. Constr Build Mater. 2019;206:297–306. https://doi.org/10.1016/j.conbuildmat.2019.02.060.
34. Menshaz MA, Johari AM, Ahmad LAZ, Characterization of metakaolin treated at different calcination temperatures. In: American Institute of Physics Conference Proceedings, pp 1892
35. Hamdy DA, Berry AS, Saleh AM, Nashwa MM. Chemical and engineering properties of blended cement containing micro and nanosilica. Am J Chem Eng. 2017;5(5):111–21. https://doi.org/10.11648/j.ajche.20170505.13.
36. Khomich VA, Emralieva SA, Tsyguleva MV. Nanosilica modifiers for cement mortar. Int Conf Oil Gas Eng. 2016;152:601–7.
37. Chen Y, Deng Y, Li M. Influence of nanosilica on the consistency, setting time, early strength, and shrinkage of composite cement paste. Adv Mater Sci Eng. 2016;2016:1–8. https://doi.org/10.1155/2016/5283706.
38. Senff L, Labrincha JA, Hotza VMD, Repette WL. Effects of nanosilica on rheology and fresh properties of cement pastes and mortars. Constr Build Mater. 2009;23:740–50. https://doi.org/10.1016/j.conbuildmat.2009.02.005.
39. Alonge OR, Mahyudden BR, Lawalson TJ. Properties of hybrid cementitious composite with metakaolin, nanosilica and epoxy. Constr Build Mater. 2017;155:740–50. https://doi.org/10.1016/j.conbuildmat.2017.08.105.
40. Naresh K. A study of metakaolin and silica fume used in various cement concrete designs. Int J Enhanc Res Sci Technol Eng. 2014;3(6):176–81.
41. Ltifi M, Guefrech A, Mounanga P, Khelidj A. Experimental study of the effect of addition of nanosilica on the behaviour of cement mortars. Engineering Procedia. 2011;10:900–5. https://doi.org/10.1016/j.proeng.2011.04.148.
42. Stat Ease. Design expert software version 13. Stat Ease Inc., Minneapolis, US. http://www.statease.com (accessed 22 September 2023)
43. Adetoro AE, Ojoawo SO, Naik P. Optimization study for bioremediation of hazardous elements from mined waste using *carica papaya* stalk actuated carbon. Mater Today Proc. 2023;88:135–43. https://doi.org/10.1016/j.matpr.2023.06.135.
44. Zhang L, Han XX, Ge J, Wang CH. The relationship between compressive and flexural strength of geopolymer grouting materials. IOP Conf Ser Mater Sci Eng. 2017;292:1–5. https://doi.org/10.1088/1757-899X/292/1/012114.
45. Shodolapo FO, Franky IK. Tensile/compressive/flexural strength relationships for concrete using kgale aggregates with botchem as binder. Int J Sci Eng Res. 2020;11:1056–63.
46. Karthiyaini S, Senthamaraikannan K, Priyadarshini J, Gupta K, Shanmugasundaram M. Prediction of mechanical strength of fiber admixed concrete using multiple regression analysis and artificial neural network. Adv Mater Sci Eng. 2019;3(6):1–7. https://doi.org/10.1155/2019/4654070.
47. Yusuf IT, Jimoh YA, Salami WA. An appropiate relationship between flexural and compressive strength of palm kernel shell concrete. Alenxandria Eng J. 2016;55:1553–62. https://doi.org/10.1016/j.aej.2016.04.008.
48. Li J, Cao J, Ren Q, Ding Y, Zhu H, Xiong C, Chen R. Effect of nanosilica and silicone of oil paraffin emulsion composite waterproofing agent on the water resistance of flue gas desulfurization gypsum. Constr Build Mater. 2021;287:1–11. https://doi.org/10.1016/j.conbuildmat.2021.123055.
49. Badogiannis E, Tsivilis S. Exploitation of poor Greek kaolins: durability of metakaolin concrete. Cem Concr Compos. 2009;31:128–33.
50. Huseien GF, Mirza J, Ismail M, Ghosal SK, Mohd Afriffin M. Effect of metakaolin replaced granulated blast furnace slag on fresh and early strength properties of geopolymer mortar. Ain Shams Eng J. 2018;9(4):1557–66.
51. Mengmeng L, Xuejiao Z, Abhijit M, Minsheng H, Varenyam A. Biomineralization in metakaolin modified cement mortar to improve its strength with lower cement content. J Hazard Mater. 2017;329:178–84.
52. Subasi A, Emiroglu M. Effects of metakaolin substitution on physical, mechanical and hydration process of white portland cement. Constr Build Mater. 2015;95:257–68.
53. Morsy MS, Al-Salloun Y, Almusallam T, Abbas H. Effect of nano metakaolin addition on the hydration characteristics of fly ash blended cement mortar. J Therm Anal Calorim. 2013;116(2):845–52. https://doi.org/10.1007/s10973-013-3512-6.

Publisher's Note Springer Nature remains neutral with regard to jurisdictional claims in published maps and institutional affiliations.